Identification of Multiple Diffusion Rates in Mixed Solvent Anion Exchange Membranes Using High Resolution MAS NMR

3 **AUTHORS**, INCLUDING:

Todd M Alam
Sandia National Laboratories

265 PUBLICATIONS **4,043** CITATIONS

Identification of Multiple Diffusion Rates in Mixed Solvent Anion Exchange Membranes Using High Resolution MAS NMR

Janelle E. Jenkins,*,[†] Michael R. Hibbs,[‡] and Todd M. Alam*,[†]

[†]Department of Electronic and Nanostructured Materials and [‡]Department of Materials, Devices, and Energy Technologies, Sandia National Laboratories, Albuquerque, New Mexico 87123, United States

S *Supporting Information*

ABSTRACT: High resolution magic angle spinning (HRMAS) ^{1}H NMR in combination with 2D exchange NOESY and pulsed field gradient (PFG) NMR diffusion experiments have been used to characterize 1 N methanol swollen polymer anion exchange membranes (AEM) presently being developed for alkaline fuel cells. Standard static ^{1}H NMR experiments on these materials have proven unsuccessful due to severe signal broadening. New experimental methods for increased resolution are needed to determine distinct solvent environments and transport properties. Using HRMAS NMR, resonances from water and methanol in both a free (bulk-like) environment and membrane-associated environment within the AEM were observed. ^{1}H HRMAS PFG NMR experiments identified different molecular diffusion environments in the solvent, while ^{1}H 2D NOESY exchange NMR experiments confirmed spatial contacts between membrane-associated species and the membrane. These results demonstrate that ^{1}H HRMAS is an ideal technique for the characterization of individual environments and diffusion rates in polymer membranes with mixed solvent systems.
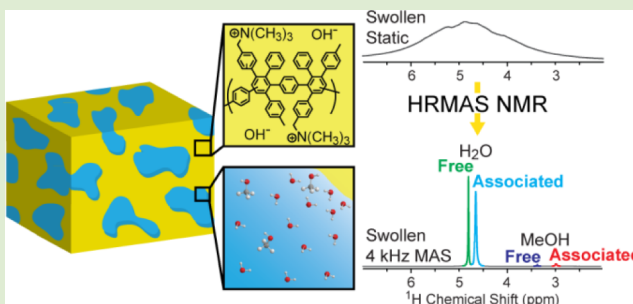
As we look at the present and toward the future, it is evident that alternative energy sources are needed. Research and advancement of fuel cell technologies is one avenue that is heavily being pursued in the race toward clean, efficient energy production. The need to extend the operating range of fuel cells is currently driving efforts toward new membrane development.[1] Many current fuel cells operate at low pH using proton exchange membranes (PEM) such as the commercially available Nafion.[2] Anion exchange membranes (AEM) are another type of polymer electrolyte being developed for applications in alkaline fuel cells.[1] AEM could potentially be utilized in high pH fuel cells. This is beneficial for direct methanol fuel cells due to the fact that methanol oxidizes more easily at higher pH.[3] Nonprecious metal catalysts can also be used at high pH, reducing the overall cost of fuel cell production.[3] The polymer−solvent interactions that occur in alkaline fuel cells are an important aspect in understanding the performance of these membrane materials. These interactions are expected to impact the observed transport properties. Due to a lack of commercial AEM there have been few fundamental studies that measure the polymer−solvent interactions.

High resolution magic angle spinning (HRMAS) NMR spectroscopy is a recently developed technique combining the power of MAS with the introduction of a magnetic field gradient along the magic angle axis. The technique narrows line widths in materials that are not pure liquid or solid by further averaging the residual dipolar interactions and removing broadening caused by magnetic susceptibility. HRMAS NMR has become very popular for studying heterogeneous soft biological samples such as tissue and lipid membranes where motional averaging is incomplete on the NMR time scale.[4−6] In addition to biological materials, HRMAS NMR can be applied to swollen resins, polymer gels and membranes, surface modified nanoparticles, and other material systems that are in the intermediate solid/liquid motional time regime.[7−18] While these examples illustrate the power of HRMAS NMR for the characterization and investigation of material systems, current applications to study polymer membranes have been limited. The coupling of HRMAS with pulsed field gradient (PFG) NMR to study diffusional processes in materials has also been reported, including the separation of different diffusion rates for mixed solvent systems in ceramics and zeolites.[9,10,19−21]

In this letter, ^{1}H HRMAS NMR is used to identify different solvent environments within the swollen anion exchange membrane, aminated tetramethyl polyphenylene (ATMPP),[22] and to provide a measurement of the diffusional processes occurring within the membrane. Figure 1a shows the static ^{1}H NMR spectra for the membrane swollen in a 1 N methanol solution. In previous studies of methanol/water swollen polymer electrolyte membranes, such as PVDFF-*g*-PSSA or Nafion 117, individual resonances for methanol and water were observed under static conditions.[23] The water and methanol species are unresolved in the static ^{1}H NMR spectrum of
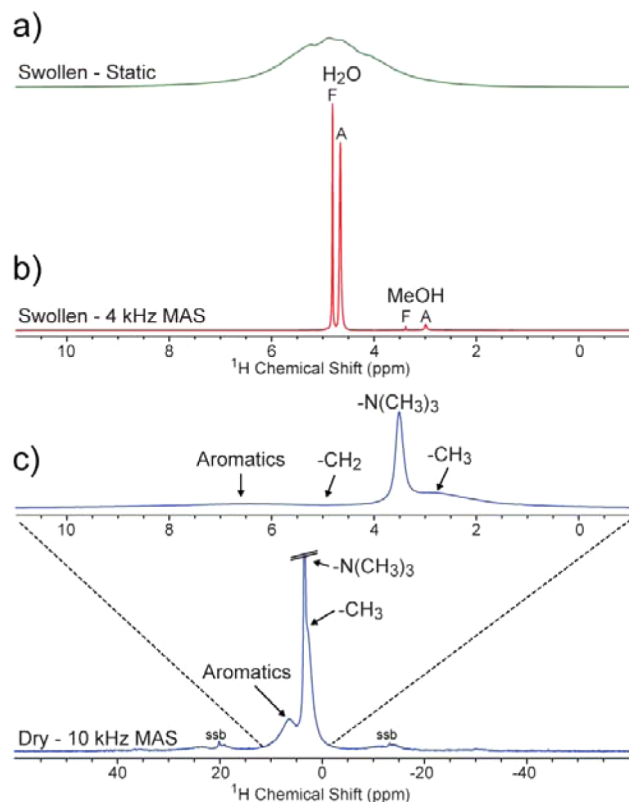
Figure 1. ^{1}H HRMAS NMR of a swollen ATMPP membrane (ion exchange capacity (IEC) = 1.45 meq/g) at static (a) and 4 kHz MAS conditions (b). Free (F) and associated (A) environments for both water and methanol are labeled. Solid state ^{1}H MAS NMR (c) of the dry membrane (free of 1 N methanol) exhibits broad resonances over a large chemical shift range that are not readily observed in the ^{1}H HRMAS spectra.

ATMPP, which exhibits a single broad resonance spanning 3−5 ppm. Under static conditions, the diffusion rate determined using PFG NMR is a weighted average of the various water and methanol environments present within the membrane and will be dominated by the water properties due to the high relative concentration.

Utilizing ^{1}H HRMAS NMR with moderate spinning speeds between 2 and 4 kHz dramatically increases the resolution of the swollen ATMPP AEM membrane, and four distinct resonances are observed (Figure 1b). These four resonances are not observed in the solid state ^{1}H MAS NMR spectrum (10 kHz) of the dried membrane free of water and methanol (Figure 1c), therefore, the resonances can be attributed to the 1 N methanol solvent in the swollen AEM. The two higher ppm

resonances in the ^{1}H HRMAS NMR of the swollen AEM (Figure 1b) are attributed to water (and the rapidly exchanging −OH from methanol), with the two lower ppm resonances being methanol. The ^{1}H MAS NMR spectrum of the dried membrane (Figure 1c) exhibits broad overlapping resonances spanning 0−10 ppm due to significant dipolar coupling, and only begins to reveal spectral resolution at spinning speeds greater than 10 kHz. The lack of a sharp aromatic signal at $\delta \sim$ +6.5 ppm in the HRMAS spectrum (Figure 1b) demonstrates that the swollen polymer does not contain regions with high polymer backbone mobility due to solvent plasticization. The methyl resonance from the polymer backbone also remains broad in the swollen polymer and cannot be readily observed in the HRMAS NMR spectra. It has been suggested that the trimethylamine side chain could become highly mobile (plasticized) in the swollen polymer leading to a resonance near $\delta \sim$ +3.5 ppm, however, at 4 kHz this resonance is not observed in the HRMAS data. In summary, for this swollen membrane system and experimental conditions, the polymer signal remains broad, is not readily observed under HRMAS, and does not bias the subsequent investigation of the sharp solvent resonances.

The chemical shift and line width of the higher ppm water and methanol resonances, as well as the fast diffusion rates observed for these environments are similar to those seen for the bulk solvent (Table 1). The resonance at δ = +4.80 ppm is therefore assigned to free or bulk-like water (F-H$_2$O), while the resonance at +3.37 ppm is consistent with the methyl protons of free methanol (F-MeOH). Based on the increased line width and the reduced diffusion rates (Table 1), the resonances at δ = +4.65 and +2.98 ppm have been assigned to water (A-H$_2$O) and methanol (A-MeOH) associated or bound to the polymer membrane, respectively.

The increased resolution observed in the ^{1}H HRMAS NMR spectra enabled ^{1}H 2D NOESY exchange experiments to be performed, which confirms the above resonance assignments. At longer mixing times (τ_{mix} > 200 ms) through-space NOE correlations were observed between the F-H$_2$O and the F-MeOH resonances (see Supporting Information), demonstrating that F-H$_2$O and F-MeOH are spatially close, which is consistent with both species being in the same free bulk-like environment. The A-H$_2$O and A-MeOH resonances also exhibit a NOE correlation at long mixing times (τ_{mix} > 200 ms), indicating that these species are also spatially close.

Broad resonances arising from the rigid membrane of the swollen AEM begin to become observable at the increased MAS rate of 6 kHz. ^{1}H 2D NOESY experiments (τ_{mix} = 500 ms) at this faster spinning speed (Figure 2a) reveal through space correlations between the A-H$_2$O (δ = +4.65 ppm)

Table 1. ^{1}H HRMAS PFG NMR Data for the ATMMP Anion Exchange Membrane (IEC = 1.45 mequiv/g)

	chemical shift (ppm)	fwhm[b] (Hz)	diffusion rate[c] (m^2/s)	χ[d]	D_{MeOH}/D_{H_2O}[e]
F-H$_2$O	4.80	8	1.8 ($\pm$0.2) $\times 10^{-9}$	0.78 $\pm$ 0.16	
A-H$_2$O	4.65	18	5.4 ($\pm$0.5) $\times 10^{-10}$	0.23 $\pm$ 0.05	
H$_2$O[a] (1 N solvent)	4.83	7	2.3 ($\pm$0.2) $\times 10^{-9}$	1	
F-MeOH	3.37	9	1.6 ($\pm$0.2) $\times 10^{-9}$	1.1 $\pm$ 0.2	0.89 $\pm$ 0.18
A-MeOH	2.98	29	2.3 ($\pm$0.2) $\times 10^{-10}$	0.15 $\pm$ 0.03	0.43 $\pm$ 0.09
MeOH[a] (1 N solvent)	3.39	2	1.5 ($\pm$0.2) $\times 10^{-9}$	1	0.65 $\pm$ 0.13

[a]The methanol and water properties measured from the 1 N solvent used to soak the membranes. [b]fwhm = full width half maximum. [c]Diffusion rate at 298 K with a diffusion delay of Δ = 50 ms. [d]χ is the measured diffusion rate of water or methanol divided by the diffusion rate of the corresponding water or methanol in the original 1 N methanol solution. [e]Ratio of diffusion rate for F-MeOH/F-H$_2$O and A-MeOH/A-H$_2$O.
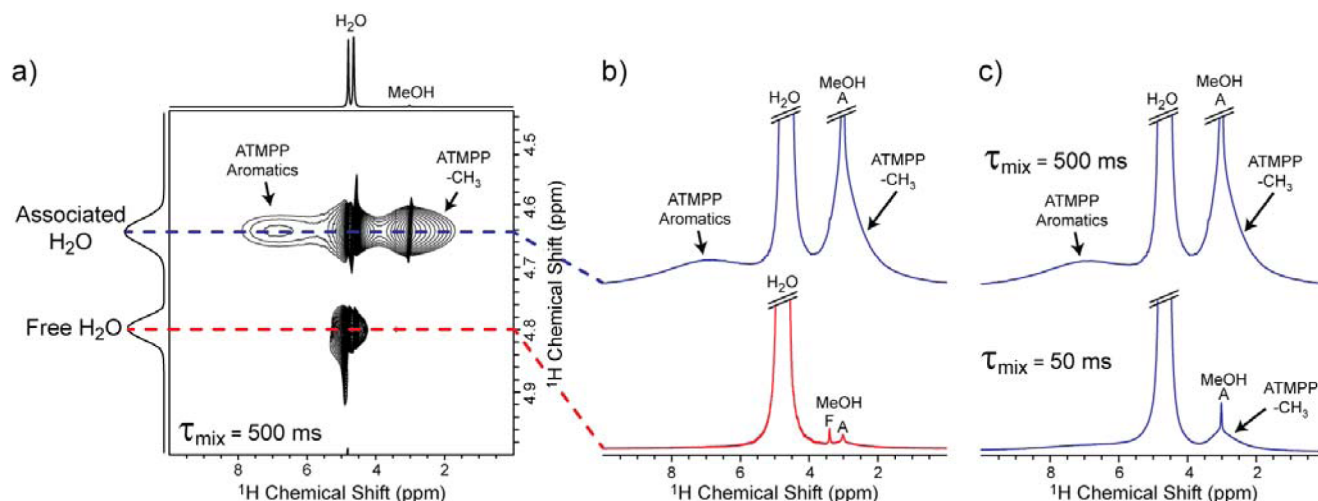
Figure 2. ^{1}H 2D NOESY exchange HRMAS NMR data (τ_{mix} = 500 ms) of 1 N methanol swollen ATMPP membrane collected at a MAS rate of 6 kHz (a). A projection taken at the A-H$_2$O resonances (δ = +4.65 ppm) shows correlations to the membrane aromatic and methyl regions (b, blue), while the projection at F-H$_2$O resonance (δ = +4.80 ppm) exhibits no correlations to the membrane (b, red). A projection at the A-H$_2$O (δ = +4.65 ppm) chemical shift with a shorter NOE mixing time (τ_{mix} = 50 ms) shows correlation to the methyl of the trimethyl amine regions of the membrane (c, bottom).

resonance and the AEM resonances at δ = +3.0 and δ = +6.9 ppm, indicating that this water environment is spatially close or associated with the polymer membrane (Figure 2b, blue). This correlation is also observed between the A-MeOH resonance (δ = +2.98 ppm) and the AEM (δ = +3.0 and +6.9 ppm, data not shown). A projection taken at the A-H$_2$O chemical shift (δ = +4.65 ppm) from ^{1}H 2D NOESY data with a shorter mixing time (τ_{mix} = 50 ms) shows that the water is predominantly located near the methyl groups of the trimethyl amines (Figure 2c, bottom). NOE correlations between the AEM and the F-H$_2$O or F-MeOH resonances were not observed (Figure 2b, red), indicating that the F-H$_2$O and F-MeOH environments are not spatially close to the membrane.

In these porous membranes the A-H$_2$O and A-MeOH species are thought to be molecules that are located near the pore walls, which contain the trimethylamine ligands, while the F-H$_2$O and F-MeOH species are envisioned to be located in the center of the pores spatially removed from the wall surface. The observation of four distinct resonances (F-H$_2$O, A-H$_2$O, F-MeOH, and A-MeOH) in swollen ATMPP is unique from previous studies on methanol/water membrane systems where only a single water and methanol resonance were observed.[23,24] The distinct water and methanol resonances observed in the swollen ATMPP membrane are not simply the result of regions within the membrane that exhibit different magnetic susceptibility as these individual associated environments reveal diffusion rates that are significantly slower than rates observed for free or bulk-like water and methanol environments (see below). Distinct water chemical shifts and diffusion constants have been reported for hydrated sulfonated naphthalenic copolyimide membranes.[25] Other studies have also argued for free and associated water environments in polymer membranes based on multiexponential diffusion behavior or differences in spin−spin T_2 and spin−lattice T_1 relaxation rates.[26,27] The current study suggests that these different solvent environments could possibly be resolved using HRMAS NMR techniques.

An upper limit on the exchange rate (k) between the free and membrane-associated sites can be estimated using the distinct chemical shifts of the free and associated water and methanol environments. The chemical shift separation between the F-

H$_2$O and A-H$_2$O is $\Delta\delta$ = 90 Hz, requiring the exchange correlation time ($\tau = 1/k$) to be significantly longer than 3.5 ms. Similarly, the chemical shift difference between the F-MeOH and A-MeOH environments was $\Delta\delta$ = 235 Hz, such that the exchange correlation time must be longer than 1.4 ms.

The integrated intensities of the water and methanol resonances were utilized to determine the solvent uptake and partitioning within the membrane. The ratio of the summation of the water peak integrals to the summation of the methanol peak integrals (F-H$_2$O + A-H$_2$O: F-MeOH + A-MeOH) is 52($\pm$6):1 and is consistent with the ratio observed in the 1 N methanol solvent (51($\pm$3):1) used to swell the AEM. This ratio demonstrates that the overall solvent uptake by the AEM membrane is nonpreferential. However, within the ATMPP membrane there is differential partitioning between the free and associated species. The ratio of F-H$_2$O to F-MeOH was 102($\pm$14):1, compared to the ratio of the A-H$_2$O to A-MeOH, which was 43($\pm$5):1, suggesting that the methanol is preferentially enriched into the membrane-associated environment of the polymer AEM. These ratios did not significantly change with spinning speed, indicating that solvent partitioning does not result from centrifugation forces that occur during sample spinning (see Supporting Information). This differential partitioning between associated and free environments may play a role in the membrane performance.

For fuel cell membranes using methanol/water solvents, it is extremely desirable to determine the transport properties for each individual solvent environment present in the membrane. The increased resolution obtained from ^{1}H HRMAS NMR enabled PFG NMR experiments to be performed using a bipolar stimulated echo (BPSTE)[28] pulse sequence to determine discrete diffusion constants of each individual solvent species within the ATMPP membrane. There are some practical aspects that must be taken into consideration when performing PFG diffusion under HRMAS conditions. Difficulties with reproducibility have been linked to sample size and are outlined nicely by Viel et al.[29] In the current investigation, a 30 μL sample volume was used to eliminate these difficulties. The diffusion results were consistent and reproducible, indicating that HRMAS diffusion measurements

on this type of membrane system are feasible. The diffusion data decay curves (Figure 3) were predominantly single
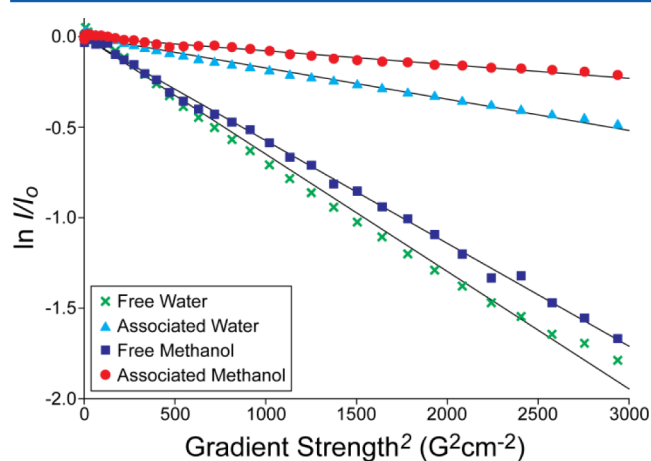
Figure 3. Normalized signal intensity decay of free and associated water and methanol environments in the ATMPP membrane as a function of gradient strength.

exponential and did not require multiexponential deconvolution. Four distinct diffusion constants are clearly observed, corresponding to the free and associated solvent environments in this swollen ATMPP AEM. These results are summarized in Table 1. Additional experimental details are provided in the Supporting Information.

The assignment of the F-H$_2$O resonance is supported by the diffusion constant for this environment as it is similar, although slightly smaller, than water in the original 1 N methanol solution. The A-H$_2$O resonance exhibits a molecular diffusion rate that is 4 times slower than water in the bulk 1 N methanol solution, consistent with water membrane surface interactions. The effective diffusion rate observed for the A-H$_2$O species represents the weighted average of the associated water diffusion rate, and the diffusion rate of the associated OH⁻ counterion (A-OH) present within the membrane (eq 1).

$$D_{eff}(\text{A-H}_2\text{O}) = \rho_{\text{A-H}_2\text{O}}D_{\text{A-H}_2\text{O}} + \rho_{\text{A-OH}}D_{\text{A-OH}} \quad (1)$$

The diffusion rate of the A-OH is predicted to be much smaller than the A-H$_2$O diffusion rate due to the strong interaction with the trimethylamine cation within the membrane. For an increasing relative fraction (ρ) of A-H$_2$O the effective diffusion rate is predicted to increase. A similar argument can be made for PEMs like Nafion or sulfonated polyethersulfone materials, but in that case the average involves the diffusion rate of the H$_3$O$^+$ cation instead of the hydroxyl diffusion rate.[30] Interestingly, recent molecular dynamic simulations for PEMs predicted that the H$_3$O$^+$ diffusion rate was not constant, but instead a function of the hydration level.[30] A similar variation with hydration level is predicted for the OH− diffusion rate in AEMs.

The methyl protons of methanol also demonstrated different diffusion rates; a rate consistent with a free or bulk-like 1 N methanol environment, and a species diffusing 7 times slower than the original 1 N methanol solution. This proportionally larger decrease in the A-MeOH diffusion rate compared to the 4 times reduction in the A-H$_2$O diffusion rate is consistent with methanol preferentially partitioning at the membrane surface. The observed self-diffusion rate of A-H$_2$O is in the range of values previously reported in AEM with similar IEC values.[31]

The A-H$_2$O and A-MeOH values (Table 1) are slightly lower than values observed for methanol and water diffusion in Nafion, ~3.5 × 10^{-10} m^2/s and ~6.5 × 10^{-10} m^2/s, respectively.[24] A group of polymer electrolytes made of poly(vinyl alcohol), sulfosuccinic acid, and poly(vinyl pyrrolidone) developed for direct methanol fuel cells exhibit diffusion rates for water that are slightly higher than A-H$_2$O of ATMPP; however, on average the A-MeOH rates in ATMPP are higher than these polymers.[32] The diffusion rate for the F-H$_2$O compared to the water diffusion rate in the 1 N solution was χ = 0.78 (Table 1), suggesting that the diffusion of free water within the pores or voids of the polymer membrane is also reduced by polymer interactions. The diffusion rates between free and associated species are also evaluated to compare to previous values. The diffusion rate ratio of F-MeOH to F-H$_2$O is 0.89 compared to 0.43 for A-MeOH to A-H$_2$O. The associated ratio is similar to ratios observed in proton-conducting membranes.[32] The lower A-MeOH to A-H$_2$O ratio (0.43) highlights the slower self-diffusion process of methanol in the membrane compared to the water and is consistent with preferential partitioning of methanol within the membrane. The Δ in the ¹H HRMAS PFG NMR experiments was also incremented to 500 ms (data not shown) to investigate the diffusion rate dependence on Δ, with no significant changes in the diffusion rates observed. The line width and chemical shifts of the individual resonances were also invariant with increasing Δ values, indicating that there were no additional overlapping spectral species present other than those already discussed, F-H$_2$O, F-MeOH, A-H$_2$O, and A-MeOH.

The ability to identify the different solvent environments present within these membranes was simply not possible using standard static ¹H NMR techniques. By applying ¹H HRMAS NMR techniques to the swollen ATMPP AEM, different solvent environments are immediately resolvable. The increased resolution enabled the measurement of individual diffusion rates for each environment, thus, providing additional insight into the transport properties of solvents within fuel cell membranes. It would be possible to obtain diffusion rates for the water and methanol components using separate ¹H and ¹³C detected PFG NMR experiments; however, the ¹³C detected PFG experiments for this sample would require up to 2 weeks instrument time, compared to the 2 h required for the ¹H detected HRMAS PFG NMR experiments utilized in this study. The increased resolution also allowed ¹H 2D NOESY exchange NMR experiments to be performed, providing spatial contacts between the solvent and membrane. Additionally, more detailed information concerning the exchange process can be obtained from the ¹H 2D NOESY exchange NMR experiments, which are currently being pursued. The ATMPP membrane characterized in this study was well suited for analyzing the different solvent environments as the membrane resonances were not readily observable at slower spinning speeds and did not interfere with the solvent characterization. However, one can imagine systems with mobile polymer resonances where the signal from the swelling solvent and membrane would overlap, and could possibly interfere with the spectral analysis. In that case diffusion filtered NMR experiments may still provide the ability to separate the membrane and solvent species.

This study furthers the applications of HRMAS NMR in materials science. It also demonstrates the benefit of this technique to the field of polymer fuel cell membranes, by enabling diffusion measurements to be performed on mixed

solvent systems which otherwise would be inaccessible with standard static NMR diffusion methods.

■ ASSOCIATED CONTENT

ⓢ Supporting Information

Additional experimental data and experimental details are supplied. This material is available free of charge via the Internet at http://pubs.acs.org.

■ AUTHOR INFORMATION

Corresponding Author

*E-mail: jejenki@sandia.gov; tmalam@sandia.gov.

Notes

The authors declare no competing financial interest.

■ ACKNOWLEDGMENTS

■ REFERENCES

(1) Zhang, H.; Shen, P. K. *Chem. Soc. Rev.* **2012**, *41*, 2382−2394.

(2) Pourcelly, G. *Pet. Chem.* **2011**, *51*, 480−491.

(3) Varcoe, J. R.; Slade, R. C. T. *Fuel Cells* **2005**, *5*, 187−200.

(4) Zietkowski, D.; Davidson, R. L.; Eykyn, T. R.; De Silva, S. S.; deSouza, N. M.; Payne, G. S. *NMR Biomed.* **2010**, *23*, 382−390.

(5) Lindon, J. C.; Beckonert, O. P.; Holmes, E.; Nicholson, J. K. *Prog. Nucl. Magn. Reson. Spectrosc.* **2009**, *55*, 79−100.

(6) Beckonert, O.; Coen, M.; Keun, H. C.; Wang, Y.; Ebbels, T. M. D.; Holmes, E.; Lindon, J. C.; Nicholson, J. K. *Nat. Protoc.* **2010**, *5*, 1019−1032.

(7) Iqbal, S.; Rodríguez-LLansola, F.; Escuder, B.; Miravet, J. F.; Verbruggen, I.; Willem, R. *Soft Matter* **2010**, *6*, 1875−1878.

(8) Sizun, C.; Raya, J.; Intasiri, A.; Boos, A.; Elbayed, K. *Microporous Mesoporous Mater.* **2003**, *66*, 27−36.

(9) Carrara, C.; Pagès, G.; Delaurent, C.; Viel, S.; Caldarelli, S. *J. Phys. Chem. C* **2011**, *115*, 18776−18781.

(10) Gratz, M.; Hertel, S.; Wehring, M.; Stallmach, F.; Galvosas, P. *New J. Phys.* **2011**, *13*, 045016.

(11) Posset, T.; Guenther, J.; Pope, J.; Oeser, T.; Blümel, J. *Chem. Commun.* **2011**, *47*, 2059−2061.

(12) Posset, T.; Blümel, J. *J. Am. Chem. Soc.* **2006**, *128*, 8394−8395.

(13) Blümel, J. *Coord. Chem. Rev.* **2008**, *252*, 2410−2423.

(14) Guenther, J.; Reibenspies, J.; Blümel, J. *Adv. Synth. Catal.* **2011**, *353*, 443−460.

(15) Siddiki, M. K.; Venkatesan, S.; Qiao, Q. *Phys. Chem. Chem. Phys.* **2012**, *14*, 4682−4686.

(16) Rousselot-Pailley, P.; Maux, D.; Wieruszeski, J.-M.; Aubagnac, J.-L.; Martinex, J.; Lippens, G. *Tetrahedron* **2000**, *56*, 5163−5167.

(17) Schröder, H. *Comb. Chem. High Throughput Screening* **2003**, *6*, 741−753.

(18) Burba, C. M.; Rice, C. V. *Mol. Cryst. Liq. Cryst.* **2012**, *555*, 280−294.

(19) Fernandez, M.; Kärger, J.; Freude, D.; Pampel, A.; van Baten, J. M.; Krishna, R. *Microporous Mesoporous Mater.* **2007**, *105*, 124−131.

(20) Fernandez, M.; Pampel, A.; Takahashi, R.; Sato, S.; Freude, D.; Kärger, J. *Phys. Chem. Chem. Phys.* **2008**, *10*, 4165−4171.

(21) Romanova, E. E.; Grinberg, F.; Pampel, A.; Kärger, J.; Freude, D. *J. Magn. Reson.* **2009**, *196*, 110−114.

(22) Hibbs, M. R.; Fujimoto, C. H.; Cornelius, C. J. *Macromolecules* **2009**, *42*, 8316−8321.

(23) Hietala, S.; Maunu, S. L.; Sundholm, F. *J. Polym. Sci., Part B: Polym. Phys.* **2000**, *38*, 3277−3284.

(24) Hallberg, F.; Vernersson, T.; Pettersson, E. T.; Dvinskikh, S.; Lindbergh, G.; Furó, I. *Electrochim. Acta* **2010**, *55*, 3542−3549.

(25) Garrido, L.; Pozuelo, J.; López-González, M.; Fang, J.; Riande, E. *Macromolecules* **2009**, *42*, 6572−6580.

(26) Volkov, V. I.; Popkov, Y. M.; Timashev, S. F.; Bessarabov, D. G.; Sanderson, R. D.; Twardowski, Z. *J. Membr. Sci.* **2000**, *180*, 1−13.

(27) Ohkubo, T.; Ohira, A.; Iwadate, Y. *J. Phys. Chem. Lett.* **2012**, *3*, 1030−1034.

(28) Cotts, R. M.; Hoch, M. J. R.; Sun, T.; Markert, J. T. *J. Magn. Reson.* **1989**, *83*, 252−566.

(29) Viel, S.; Ziarelli, F.; Pagès, G.; Carrara, C.; Caldarelli, S. *J. Magn. Reson.* **2008**, *190*, 113−123.

(30) Ohkubo, T.; Kidena, K.; Takimoto; Ohira, A. *J. Mol. Model.* **2012**, *18*, 533−540.

(31) Hibbs, M. R.; Hickner, M. A.; Alam, T. M.; McIntyre, S. K.; Fujimoto, C. H.; Cornelius, C. *J. Chem. Mater.* **2008**, *20*, 2566−2573.

(32) Huang, Y. F.; Chuang, L. C.; Kannan, A. M.; Lin, C. W. *J. Power Sources* **2009**, *186*, 22−28.